



HAL
open science

New insights on the electronic, magnetic, electric and molecular structure of a bis-(4-cyanopyridine) iron(III) complex with the meso-tetrakis(4-methoxyphenyl)porphyrin

Leila Ben Haj Hassen, Selma Dhifaoui, Yoann Rousselin, Valérie Marvaud, Christine Stern, Charles Schulz, Habib Nasri

► **To cite this version:**

Leila Ben Haj Hassen, Selma Dhifaoui, Yoann Rousselin, Valérie Marvaud, Christine Stern, et al.. New insights on the electronic, magnetic, electric and molecular structure of a bis-(4-cyanopyridine) iron(III) complex with the meso-tetrakis(4-methoxyphenyl)porphyrin. *Inorganica Chimica Acta*, 2019, 486, pp.675-683. 10.1016/j.ica.2018.11.040 . hal-02397976

HAL Id: hal-02397976

<https://hal.sorbonne-universite.fr/hal-02397976v1>

Submitted on 6 Dec 2019

HAL is a multi-disciplinary open access archive for the deposit and dissemination of scientific research documents, whether they are published or not. The documents may come from teaching and research institutions in France or abroad, or from public or private research centers.

L'archive ouverte pluridisciplinaire **HAL**, est destinée au dépôt et à la diffusion de documents scientifiques de niveau recherche, publiés ou non, émanant des établissements d'enseignement et de recherche français ou étrangers, des laboratoires publics ou privés.

New insights on the electronic, magnetic, electric and molecular structure of a bis-(4-cyanopyridine) iron(III) complex with the *meso*-tetrakis(4-methoxyphenyl)porphyrin



Leila Ben Haj Hassen^a, Selma Dhifaoui^a, Yoann Rousselin^b, Valérie Marvaud^c, Christine Stern^d, Charles E. Schulz^e, Habib Nasri^{a,*}

^a Laboratoire de Physico-chimie des Matériaux, Faculté des Sciences de Monastir, Avenue de l'environnement, University of Monastir, 5019 Monastir, Tunisia

^b ICMUB, UMR CNRS 6302, Université Bourgogne Franche-Comté, 9 avenue Alain Savary, 21078 Dijon cedex, France

^c IPCM, Institut Parisien de Chimie Moléculaire, UPMC, Sorbonne Université, 4 Place Jussieu, 75252 Paris Cedex 05, France

^d Université de Bourgogne Franche-Comté, ICMUB (UMR CNRS 6302), 9 Avenue Alain Savary, BP 47870, 21078 Dijon Cedex, France

^e Department of Physics, Knox College, Galesburg, IL 61401, USA

ARTICLE INFO

Keywords:

Iron(III) porphyrin
X-ray Molecular structure
Magnetic properties
Cyclic voltammetry

ABSTRACT

We have successfully synthesized and characterized a new low-spin iron(III) bis(4-cyanopyridine) complex with a *meso*-porphyrin substituted in the *para* positions of the phenyls by the methoxy group, namely the bis(4-cyanopyridine)[(*meso*-tetrakis(4-methoxyphenylporphyrinato)]iron(III) trifluoromethanesulfonate chlorobenzene monosolvate complex with the formula $[\text{Fe}^{\text{III}}(\text{TMPP})(4\text{-CNpy})_2]\text{SO}_3\text{CF}_3 \cdot \text{C}_6\text{H}_5\text{Cl}$ (I). This species was characterized through ultraviolet-visible, Fourier-transform infrared and Mössbauer spectroscopy as well as by SQUID magnetometry, cyclic voltammetry, and X-ray crystallography. These characterizations indicated that our synthetic heme model is a low-spin ($S = 1/2$) coordination compound and especially shows that the structural, electronic and the magnetic properties of complex (I) are closely dominated by the presence of the methoxy σ -donor group at the *para* positions of the *meso*-porphyrin.

1. Introduction

An exceedingly important group of heme proteins is made by hexa-coordinated heme species with two axial histidines as the fifth and sixth ligands. Among them are cytochromes which are heme proteins involved in electronic transfer such as cytochrome *c*3 [1], cytochromes *b*4 [2] and cytochrome *b*5 [3]. The cytochrome *b*5 and three of the four hemes of the cytochrome *c*3 have the imidazole rings of the two coordinated histidines in nearly parallel orientation, while in the cytochrome *c*3, the imidazole planes are nearly perpendicular. Additionally, there are a number of membrane cytochromes *b* with bis(histidine) ligands including the two cytochromes *b* known as the ubiquinone-cytochrome *c* – cytochrome *c* oxidoreductase and the chloroplast cytochrome *b*6 [4]. For these iron(III) biological derivatives, there is a correlation between the axial ligand plane orientation and the reduction potentials as reported by Niki et al., [5]. The relative orientation of the two imidazole planes with respect to each other is important to understand the redox and the spectroscopic properties of these types of heme proteins.

It is noteworthy that for more than a half century, iron(III) porphyrin synthetic complexes have been used as models for heme proteins. This is very suitable because they can be characterized by different techniques such as Mössbauer, EPR, Raman, NMR spectroscopy, cyclic voltammetry and X-ray molecular structures. These measurements can be done much more easily and with a better resolution data than for hemoproteins. Indeed, synthetic models made by iron(III) hexa-coordinated metalloporphyrins with planar bis(*N*-donor) planar axial ligands have been intensively investigated. This is the case of bis(imidazole), bis(substituted imidazoles), bis(pyridine) and bis(substituted pyridines) iron(III) porphyrin coordination compounds [6–9].

For these hexa-coordinated iron(III) species, the orientations of the two trans planar axial ligands have been intensively investigated especially by Safo et al., [10,11]. These structural, EPR and Mössbauer studies showed that the relative orientations of the axial ligands have an important effect on the electronic structures of these species. These and other studies [11,12] indicated that there are two types of electronic configurations of the ground state of the low-spin ($S = 1/2$) iron(III) for $[\text{Fe}^{\text{III}}(\text{Porph})(\text{L})]^+$ ion complexes where L is a *N*-donor planar

* Corresponding author.

E-mail addresses: habib.nasri@fsm.rnu.tn, hnasri1@gmail.com (H. Nasri).

axial ligand. These are: $(d_{xy})^2(d_{xz}, d_{yz})^2$ known as the axial electronic configuration or the classic configuration and $(d_{xz}, d_{yz})^4(d_{xy})^1$ known as the novel electronic configuration.

The three major factors that affect the electronic ground state of these iron(III) metalloporphyrins are: (i) electron withdrawing groups at the *meso*-positions of the porphyrin stabilize the $(d_{xy})^2(d_{xz}, d_{yz})^2$ ground state configuration, while donating groups stabilize the $(d_{xz}, d_{yz})^4(d_{xy})^1$ ground state configuration; (ii) axial ligands with strong π -accepting character stabilize the $(d_{xz}, d_{yz})^4(d_{xy})^1$ ground state while those with strong σ -donating and π -donating ability stabilize the $(d_{xy})^2(d_{xz}, d_{yz})^2$ ground state; and (iii) strong deformation, especially the ruffling distortion, of the porphyrin macrocycle stabilizes the $(d_{xz}, d_{yz})^4(d_{xy})^1$ ground state electronic configuration.

The 4-cyanopyridine (4-CNpy) is known as a strong π -acceptor N-donor planar axial ligand and in the literature, only the molecular structures of two iron(III) bis(4-CNpy) porphyrin ion complexes are known: the bis(4-cyanopyridine)(*meso*-tetraphenylporphyrinato)iron(III) perchlorate with the formula $[\text{Fe}^{\text{III}}(\text{TPP})(4\text{-CNpy})_2]\text{ClO}_4$ [11] and the bis(4-cyanopyridine)(*meso*-tetramesitylphenylporphyrinato)iron(III) perchlorate with the formula $[\text{Fe}^{\text{III}}(\text{TMP})(4\text{-CNpy})_2]\text{ClO}_4$ [10].

On the other hand, in 1996, Walker et al., [13] reported the redox properties and the thermodynamic stabilities of several iron(III) bis(4-CNpy) derivatives with different phenyls substituted at the *ortho* positions of *meso*-porphyrins with OCH_3 , F, Cl, Br and CH_3 groups. Nevertheless, a completed investigation of an iron(III) bis(4-CNpy) heme model including UV-visible, IR, Mössbauer, cyclic voltammetry and magnetic investigations has not yet been reported in the literature. In an attempt to obtain further information about the role of 4-cyanopyridine ligand as well as the nature of the substituted group on the phenyl rings of the *meso*-porphyrin on the structural, electronic and the magnetic properties of cytochromes, we synthesized and fully characterized the bis(4-cyanopyridine)[(*meso*-tetrakis(4-methoxyphenylporphyrinato)]iron(III) trifluoromethanesulfonate chlorobenzene monosolvate complex (I). On the other hand, even though the major investigations involving iron(III) metalloporphyrins have been undertaken due to the fact that these species are very good models for heme proteins, these coordination compounds are also known to be good catalysts for several organic and inorganic reactions [14–17] and these coordination compounds are actually used in several domains such as chemical sensors [18–20].

2. Experimental section

2.1. Materials and methods

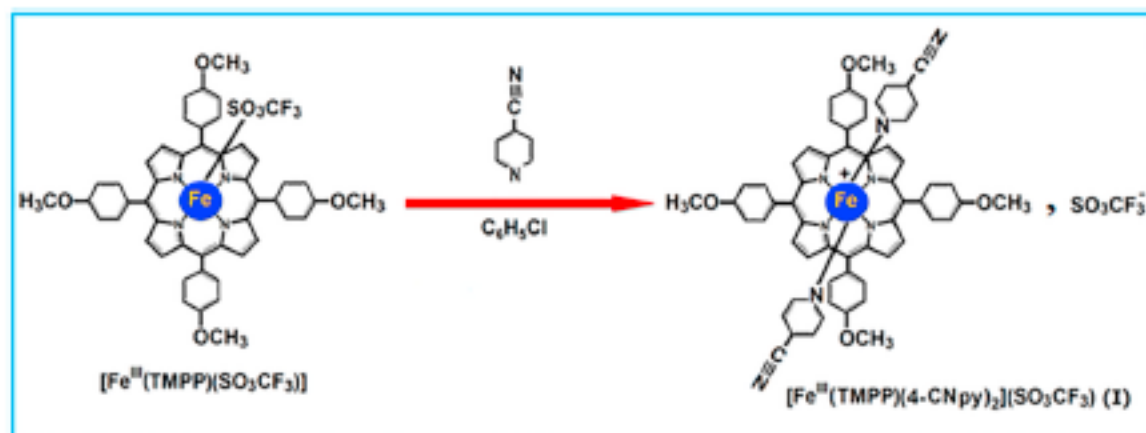
All solvents and reagents were purchased from commercial supplies and used without further purifications and all manipulations were carried out under aerobic conditions. The *meso*-tetrakis(4-methoxyphenyl)porphyrin (H_2TMPP) was prepared by using the Alder and

Longo method [21] and the triflate iron(III) porphyrin starting material $[\text{Fe}^{\text{III}}(\text{TMPP})(\text{SO}_3\text{CF}_3)]$ has been prepared using the literature reported method [22].

Fourier-transform IR spectra were recorded on a PerkinElmer Spectrum Two FT-IR spectrometer. UV/Vis spectra were recorded with a WinASPECT PLUS (validation for SPECORD PLUS version 4.2). Scanning spectrophotometer mass spectra were recorded with a Bruker autoflex III smartbeam instrument (ESI, positive mode). Cyclic voltammetry (CV) experiments were performed with a CH-660B potentiostat (CH Instruments). All analytical experiments were conducted at room temperature under an argon atmosphere in a standard one-compartment, three-electrode electrochemical cell. Tetra-*n*-butylammoniumhexafluorophosphate (TBAPF_6) was used as the supporting electrolyte (0.2 M) in dichloromethane previously distilled over calcium hydride under argon. An automatic Ohmic drop compensation procedure was systematically implemented before the CV data were recorded with electrolytic solutions containing the compounds under study at concentrations of ca. 10^{-2} M. CH Instruments vitreous carbon ($\phi = 2$ mm) working electrodes were polished with 1 μm diamond paste before each recording. The saturated calomel electrode SCE (TBAPF_6 0.2 M in CH_2Cl_2) redox couple was used as the reference electrode. The potential of the ferrocene/ferrocenium redox couple was used as an internal reference (0.47 V/SCE experimental conditions). All potentials are given vs SCE. Temperature-dependent magnetic susceptibility measurements on polycrystalline samples of (I) were carried out on a Quantum Design MPMS SQUID susceptometer equipped with a 7 T magnet and operating in the range of temperature from 1.8 to 400 K. The compacted powdered samples were placed in a diamagnetic sample holder and the measurements were carried out in a 1000 Oe applied field using the extraction technique. Magnetization versus magnetic field measurements of (I) were carried out at 2 K in the field range 0–5 T. The amount of material used for the measurements was 11.59 mg for (I). Before analysis, the experimental susceptibility was corrected from the sample holder. Diamagnetic corrections of the constituent atoms of (I) were estimated from Pascal constants [23] with the value -295×10^{-6} .

2.2. Syntheses of $[\text{Fe}^{\text{III}}(\text{TMPP})(4\text{-CNpy})_2](\text{SO}_3\text{CF}_3) \cdot \text{C}_6\text{H}_5\text{Cl}$ (I)

$[\text{Fe}^{\text{III}}(\text{TMPP})(\text{SO}_3\text{CF}_3)]$ (50 mg, 0.05 mmol) and 4-cyanopyridine (90 mg, 0.064 mmol) in 25 mL of chlorobenzene were stirred overnight at room temperature. The color of the reaction mixture changed from brown-red to blood-red and crystals of the bis(4-cyanopyridine)[(*meso*-tetrakis(4-methoxyphenylporphyrinato)]iron(III) trifluoromethanesulfonate chlorobenzene monosolvate complex $[\text{Fe}^{\text{III}}(\text{TMPP})(4\text{-CNpy})_2](\text{SO}_3\text{CF}_3) \cdot \text{C}_6\text{H}_5\text{Cl}$ (I) (4-CNpy = 4-cyanopyridine) were prepared by slow diffusion of *n*-hexane into the chlorobenzene solution (Scheme 1). Anal. Calc. for (I), $\text{C}_{67}\text{H}_{49}\text{ClF}_3\text{FeN}_6\text{O}_7\text{S}$ (1258.53 g/mol): C, 63.94; H, 3.92; N, 8.90%. Found:



Scheme 1. Synthesis of $[\text{Fe}^{\text{III}}(\text{TMPP})(4\text{-CNpy})_2](\text{SO}_3\text{CF}_3) \cdot \text{C}_6\text{H}_5\text{Cl}$ (I).

C, 64.26; H, 4.03; N, 8.7996. UV-visible [C_6H_5Cl λ_{max} in nm (log ϵ): 417 (4.87), 509 (3.65), 572 (3.45). IR (solid, cm^{-1}): $\nu = 3057$ w, 2926 w, 2836 w, 2240 w, 1607 m, 1510 m, 1240 s, 1176 s, 1022 s, 806 s, 624 s, 553 m. MS (MALDI-TOF) m/z : 788.10 $[Fe(TMPP)]^+$, 814.12 $[Fe(TMPP)(CN)]^+$, 890.24 $[Fe(TMPP)(4-CNpy) + 2H]^+$.

2.3. Crystallography

A dark blue crystal of $[Fe^{III}(TMPP)(4-CNpy)_2](SO_2CF_3)_2 \cdot C_6H_5Cl$ (I) was used for the X-ray structure determination. Data collection was carried out on a Nonius Kappa, APEX II diffractometer equipped with a graphite-monochromated Mo-K α radiation source ($\lambda = 0.71073 \text{ \AA}$). The intensity data for this compound were collected by the narrow-frame method at low temperature (115 K). The unit-cell parameters were calculated and refined from the full data set. The reflections were scaled and corrected for absorption effects with the SADABS program [24]. Using Olex2 [25], the structure was solved with the Superflip [26] structure solution program using the charge flipping solution method. The model was refined with the SHELXL [27] refinement package using least squares minimization. The molecular graphics were drawn using ORTEP-3 for Windows [28]. H-atoms were positioned geometrically and refined using a riding model with C-H = 0.95, 0.98 and 0.99 \AA and N-H = 0.92 \AA with $U_{iso}(H_{phenyl, methyl}) = 1.2U_{eq}(C/N)$ and $U_{iso}(H_{methyl}) = 1.5U_{eq}(C)$. All non-hydrogen atoms were refined anisotropically. In the final difference Fourier map, the highest peak is 0.47 and the deepest hole is -0.65. Crystallographic data and structure refinement of $[Fe^{III}(TMPP)(4-CNpy)_2](SO_2CF_3)_2 \cdot C_6H_5Cl$ (I) are given in Table 1 and selected bond distances and angles for this iron(III) derivative are listed in Table SI-1 (supplementary information).

Table 1
Crystal data and structural refinement for $[Fe^{III}(TMPP)(4-CNpy)_2](SO_2CF_3)_2 \cdot C_6H_5Cl$ (I).

Formula	$C_{67}H_{46}ClF_6FeN_8O_7S$
$D_{calc}/g\text{ cm}^{-3}$	1.410
μ/mm^{-1}	0.408
Formula Weight	1258.53
Color	Dark blue
Shape	Prism
Size/ mm^3	$0.50 \times 0.40 \times 0.15$
T (K)	115
Crystal System	Monoclinic
Space Group	$P2_1/c$
a (\AA)	20.4813(13)
b (\AA)	17.5063(10)
c (\AA)	24.3614(16)
α ($^\circ$)	90
β ($^\circ$)	137.268(2)
γ ($^\circ$)	90
V (\AA^3)	5927.3(7)
Z	4
R_{int} ($^\circ$)	0.812
R_{max} ($^\circ$)	0.941
Reflections measured	67,061
Independent reflections	11,617
Observed reflections [$I > 2\sigma(I)$]	8017
R_{int}	0.0536
Parameters	798
Largest Peak	0.470
Deepest Hole	-0.650
Goof	1.077
wR_2 (all data)	0.1301
wR_2 [$I > 2\sigma(I)$] ^{a,b}	0.1117
R_1 (all data)	0.0884
R_1 [$I > 2\sigma(I)$] ^{a,b}	0.0485

^a : $wR_2 = \{\sum[w(F_o^2 - F_c^2)^2]/\sum[w(F_o^2)^2]\}^{1/2}$.

^b : $R_1 = \sum||F| - |F_c||/\sum|F_o|$.

3. Results and discussion

3.1. UV-visible and IR data

The electronic spectra of compound (I) and the starting material complex $[Fe^{III}(TMPP)(SO_2CF_3)]$ are illustrated in Fig. 1. The positions of the Soret and the Q bands of the iron(III)-bis(4-CNpy) derivative are red-shifted vis-à-vis of the iron(III)-triflate starting material. Indeed, the value of the λ_{max} of the Soret band is 417 nm which is redshifted compared to that of the triflate starting material (405 nm). For the two related species $[Fe^{III}(TPP)(4-CNpy)_2]^+$ (TPP: *meso*-tetraphenylporphyrinato) [11] and $[Fe^{III}(TMP)(4-CNpy)_2]^+$ (TMP = *meso*-tetramesitylphenylporphyrinato) [10], the values of the λ_{max} of the Soret band are 416 nm and 412 nm respectively which are quite close to those of our bis(4-CNpy)-TMPP derivative.

As it will be shown in the crystallographic section, the macrocycles of the three iron(III)-bis(4-CNpy) species with the TPP, TMP and TMPP moieties are ruffled, as a consequence, one can expect that we must observe an important redshift of the Soret bands of these iron(III) metalloporphyrins [29] which is not the case where the λ_{max} of the Soret bands of these three species are ~ 415 nm. In the case of the later reference, the iron(III) chloro complex $[Fe^{III}(DPP)Cl]$ where DPP is the 2,3,7,8,12,13,17,18-octaphenyl-5,10,15,20-tetraphenylporphyrinato (or the dodecaphenylporphyrinato) which is a *meso*-phenylporphyrin with a phenyl group in the eight β -pyrrolic positions. This species which exhibits a very high ruffled and saddled, shows a very redshifted Soret band at 444 nm compared to 418 nm for the $[Fe^{III}(TPP)Cl]$ complex [30] (Table SI-2). By the other hand, we recently reported that, the oxovanadyl species $[V(TTP)O]$ with the *meso*-tetratolyleporphyrinato (TTP) presents a Soret band at 426 nm while for the related compound $[V(Cl_8TTP)O]$ where the Cl₈TTP is the TTP *meso*-porphyrinato with the eight β -pyrrolic positions occupied by chlorine atoms, the Soret band is 451 nm. The later derivative exhibits a very important deformation of the porphyrin core [31].

It is clear from what we just mentioned above that, the important redshift of the Soret band is mainly due to the bulkiness of the β -pyrrole groups (a phenyl group or a halide group for examples) which lead to an important steric interaction between these groups and the phenyls at the *meso* positions of the porphyrin. This deduction was also mentioned by Jiang et al., [32].

By the other hand, the optical gap (Eg-op) which corresponds to the energy difference between the levels of the HOMO and LUMO orbitals

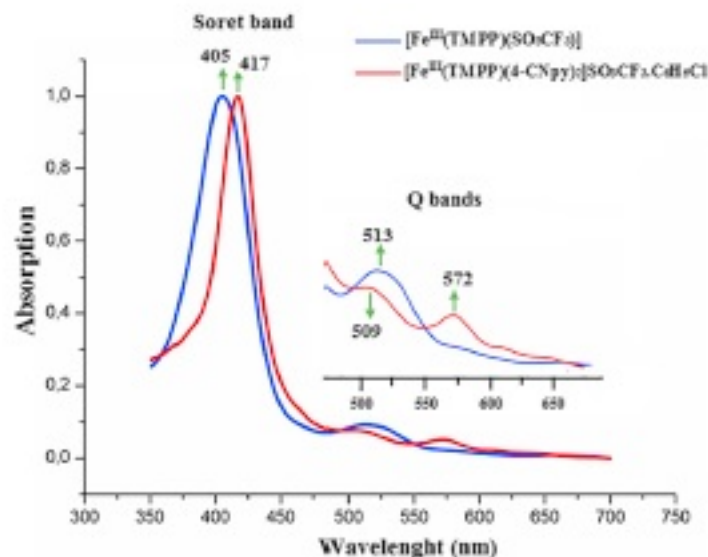


Fig. 1. UV-visible absorption spectra of the $[Fe^{III}(TMPP)(SO_2CF_3)]$ starting material and $[Fe^{III}(TMPP)(4-CNpy)_2](SO_2CF_3)_2 \cdot C_6H_5Cl$ (I). Spectra are recorded in CH_2Cl_2 solution at concentrations $\sim 10^{-6}$. The inset shows enlarged view in the Q bands region.

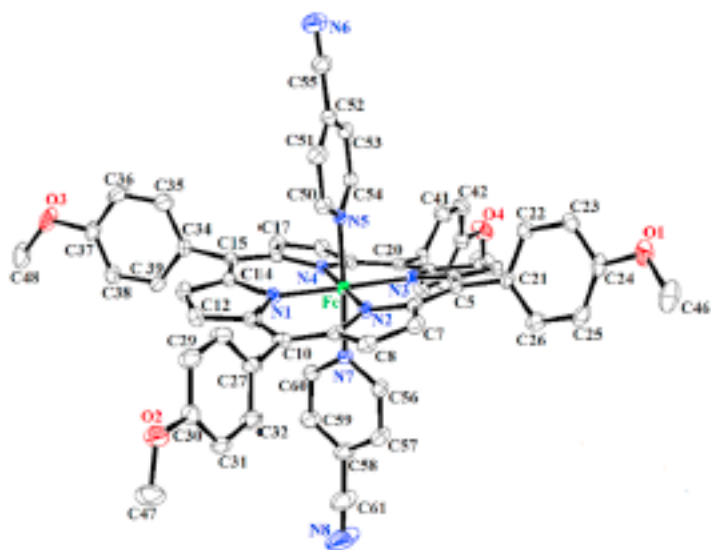


Fig. 2. ORTEP diagrams of the $[\text{Fe}^{\text{III}}(\text{TMPP})(4\text{-CNpy})_2]^+$ ion complex. Ellipsoids are drawn at 40%. The hydrogen atoms are omitted for clarity.

of the porphyrin was obtained using the Tauc plot method. The value of the Eg-op obtained for (I) is 1.71 eV which is in the normal range of meso-porphyrin complexes.

The IR spectrum of (I) shows that the $\nu(\text{C}\equiv\text{N})$ stretching frequency value of the 4-cyanopyridine axial ligand is 2240 cm^{-1} which is slightly below that of the free ligand (2243 cm^{-1}) indicating that the 4-CNpy ligand is coordinated to the iron through the pyridyl group and not the nitrile moiety.

Table 2

Selected structural features of (I) and several iron(III) metalloporphyrins.

Complex	Fe-Np ^a (Å)	Fe-Lax ^b (Å)	ϕ (°) ^c	φ (°) ^d	$10^2 \Delta C_{\text{meso}}^e$	Spin state	Ref.
Iron(III) high-spin ($S = 5/2$) porphyrins							
$[\text{Fe}^{\text{III}}(\text{TPP})\text{Cl}]^f$	2.070(9)	2.211(1)	–	–	–	5/2	[36]
$[\text{Fe}^{\text{III}}(\text{TTP})(\text{OAc})]^{g,h}$	2.067(4)	1.898(4)	–	–	–	5/2	[37]
$[\text{Fe}^{\text{III}}(\text{TpivPP})(\text{NCO})]^i$	2.069(5)	1.970(5)	–	–	–	5/2	[38]
$[\text{Fe}^{\text{III}}(\text{TPP})(\text{H}_2\text{O})_2]^{+j}$	2.045	2.095	–	–	–	5/2	[39]
$[\text{Fe}^{\text{III}}(\text{OEP})(\text{NCS})(\text{py})]^l$	2.048	2.031/2.442	–	–	–	5/2	[40]
$[\text{Fe}^{\text{III}}(\text{TPP})(\text{F})_2]^{+j}$	2.064	1.966	–	–	–	5/2	[41]
$[\text{Fe}^{\text{III}}(\text{OEP})(\text{DMSO})_2]^{+k}$	2.037	2.083	–	–	–	5/2	[42]
Iron(III) low-spin ($S = 1/2$) porphyrins							
$[\text{Fe}^{\text{III}}(\text{TPP})(4\text{-CNpy})_2]^{+l}$	1.952(7)	1.997(4)/2.008(4)	88.97	37/36	55	1/2	[11]
$[\text{Fe}^{\text{III}}(\text{TMP})(4\text{-CNpy})_2]^l$	1.961(6)	2.021(6)/2.001(5)	87.4	43/44	41	1/2	[10]
$[\text{Fe}^{\text{III}}(\text{TMP})(4\text{-NMe}_2\text{py})_2]^{+m,n}$	1.964(10)	1.989(4)/1.978(4)	78.84	37/42	51	1/2	[10]
$[\text{Fe}^{\text{III}}(\text{TMP})(3\text{-Clpy})_2]^{+l,o}$	1.968(2)	2.012(8)	76.94	29/41	36	1/2	[10]
$[\text{Fe}^{\text{III}}(\text{TPP})(2\text{-MeHIm})_2]^{+p,q}$	1.970	2.012	–	–	39	1/2	[43]
$[\text{Fe}^{\text{III}}(\text{TMPP})(4\text{-CNpy})_2]^+$	1.971(2)	2.008(2)/2.006(2)	72.6	37/35	21	1/2	This work
$[\text{Fe}^{\text{III}}(\text{TPP})(\text{py})_2]^{+r}$	1.982	2.005/2.001	86	52	25	1/2	[8]
$[\text{Fe}^{\text{III}}(\text{TPP})(\text{HIm})_2]^{+s,t}$	1.993	1.964	–	–	–	1/2	[7]
$[\text{Fe}^{\text{III}}(\text{TPP})(\text{CN})_2]^{-t}$	2.000	1.975	–	–	Planar core	1/2	[44]

^a : Fe-Np = average equatorial distance between the iron and the nitrogen atoms of the porphyrin ring.

^b : Fe-Lax = iron-axial ligand distance.

^c : ϕ = dihedral angle between the two planes of the axial ligands.

^d : φ = the smallest dihedral angle between the Np-Fe-Np vector and the projection of the pyridyl plane of the 4-CNpy ligand in the porphyrin macrocycle.

^e : ΔC_{meso} = The average absolute displacement values of the meso carbon with respect to the plan of the 24 atoms of the porphyrin core.

^f : TPP = meso-tetraphenylporphyrinato.

^g : TTP = meso-tetratolylphenylporphyrinato.

^h : OAc = acetato.

ⁱ : TpivPP = α,α,α -tetrakis(*o*-pivalamidophenyl)porphyrinato.

^j : OEP = octaethylporphyrinato.

^k : DMSO = dimethylsulfoxide.

^l : TMP = meso-tetramesitylporphyrinato.

^m : 4-NMe₂Py = 4-(dimethylamino)pyridine.

ⁿ : 3-Clpy = 3-cyanopyridine.

^o : 2-MeHIm = 2-methylimidazole.

^p : HIm = imidazole.

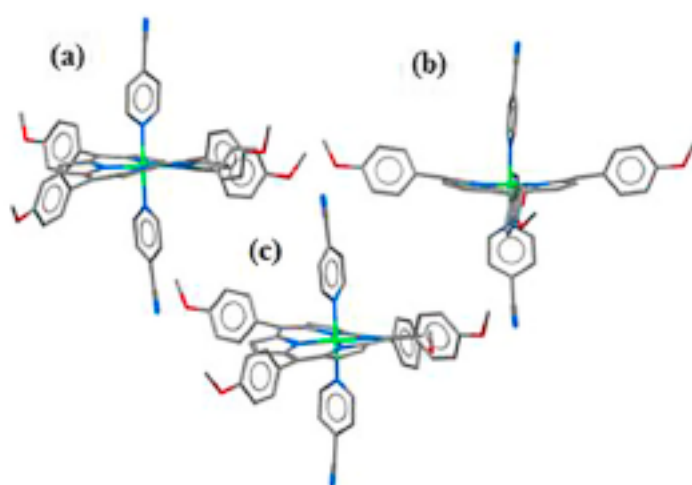


Fig. 3. Drawings (a), (b) and (c) showing the important ruffle deformation of the porphyrin core of the ion complex $[\text{Fe}^{\text{III}}(\text{TMPP})(4\text{-CNpy})_2]^+$ (I).

3.2. Structural properties of $[\text{Fe}^{\text{III}}(\text{TMPP})(4\text{-CNpy})_2](\text{SO}_2\text{CF}_3)\cdot\text{C}_6\text{H}_5\text{Cl}$ (I)

The structure of $[\text{Fe}^{\text{III}}(\text{TMPP})(4\text{-CNpy})_2](\text{SO}_2\text{CF}_3)\cdot\text{C}_6\text{H}_5\text{Cl}$ (I) has been determined at 115(2) K. Fig. 2 is an ORTEP diagram of the $[\text{Fe}^{\text{III}}(\text{TMPP})(4\text{-CNpy})_2]^+$ cation. The asymmetric unit of (I) contains one $[\text{Fe}^{\text{III}}(\text{TMPP})(4\text{-CNpy})_2]^+$ ion complex, one SO_2CF_3^- counterion and one chlorobenzene solvent molecule. The iron(III) cation is chelated by four pyrrole-N atoms of the porphyrinate anion and coordinated by two pyridyl-N atoms of the two 4-CNpy trans axial ligands in a distorted octahedral geometry.

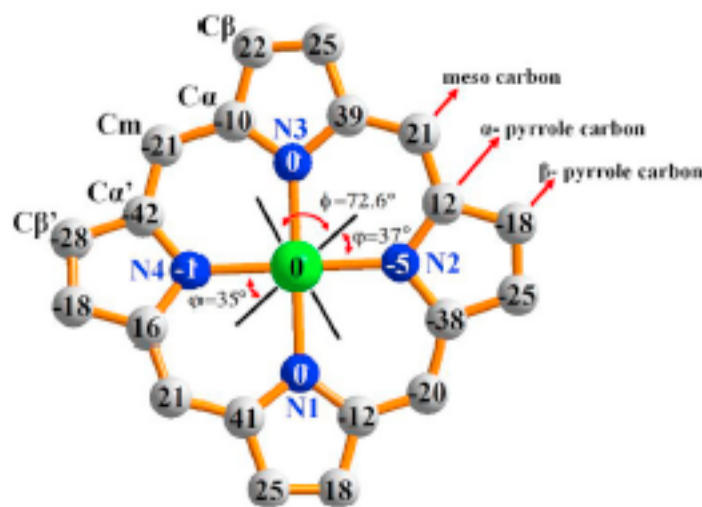


Fig. 4. Formal diagrams of the porphyrinato cores of (I). The displacements of each atom from the 24-atom core plane in units of 0.01 Å are also illustrated. The diagram shows also the ϕ angle values between the axial 4-CNpy ligands and the closest N(pyrrole)-Fe-N(pyr) plane and also the dihedral angle ϕ between the two axial planar ligands.

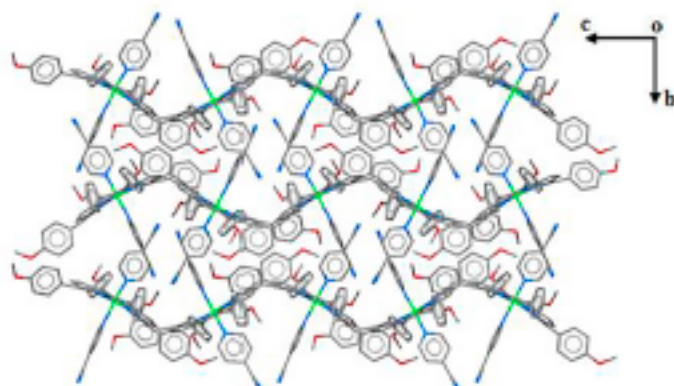


Fig. 5. The crystal packing of (I), viewed along the [100] direction. The SO_2CF_3^- counterions and the chlorobenzene solvent molecules are omitted for clarity.

It has been shown that the value of the average equatorial iron-pyrrole N atoms distance (Fe-Np) and the spin-state of the iron(III) porphyrin complexes are related [33]. For iron(III) high-spin ($S = 5/2$) metalloporphyrins, the value of the Fe-Np bond length are high and > 2.035 Å or longer, while low-spin ($S = 1/2$) iron(III) porphyrin derivatives exhibit smaller values of Fe-Np distances in the range [1.998–1.950] Å (Table 2).

Scheidt and Walker [11] reported that low-spin iron(III) metalloporphyrins of type $[\text{Fe}^{\text{III}}(\text{Porph})(\text{L})_2]^+$ (Porph = porphyrinato and L is a neutral planar N-donor axial ligand) exhibit two ground state electronic configurations of Fe(III): $(d_{xy})^2(d_{xz}, d_{yz})^2$ and $(d_{xz}, d_{yz})^4(d_{xy})^1$. The first configuration, known as the classic configuration, has been shown for $[\text{Fe}^{\text{III}}(\text{Porph})(\text{L})_2]^+$ species with nearly parallel planes for axial ligands L which are reasonably strong σ and π -donors such as the imidazole and DMAP (4-(N,N-dimethylamino)pyridine) [34]. The strong π -acceptor L axial ligands such as pyridine exhibit the novel $(d_{xz}, d_{yz})^4(d_{xy})^1$ electronic configuration of the ground state of the iron(III) cation. In the case of strong π -acid axial ligand, the central metal must π -donate electron density to the axial ligand, consequently the iron(III) must be a good π -acceptor from the π -donating porphyrinato moiety [11]. As a consequence of the π interaction between the central metal and the nitrogen atoms of the porphyrin, the Fe-Np equatorial distance will decrease, which is possible when the porphyrin core is strongly ruffled. This feature was first noted by Hoard more than four decades ago [35].

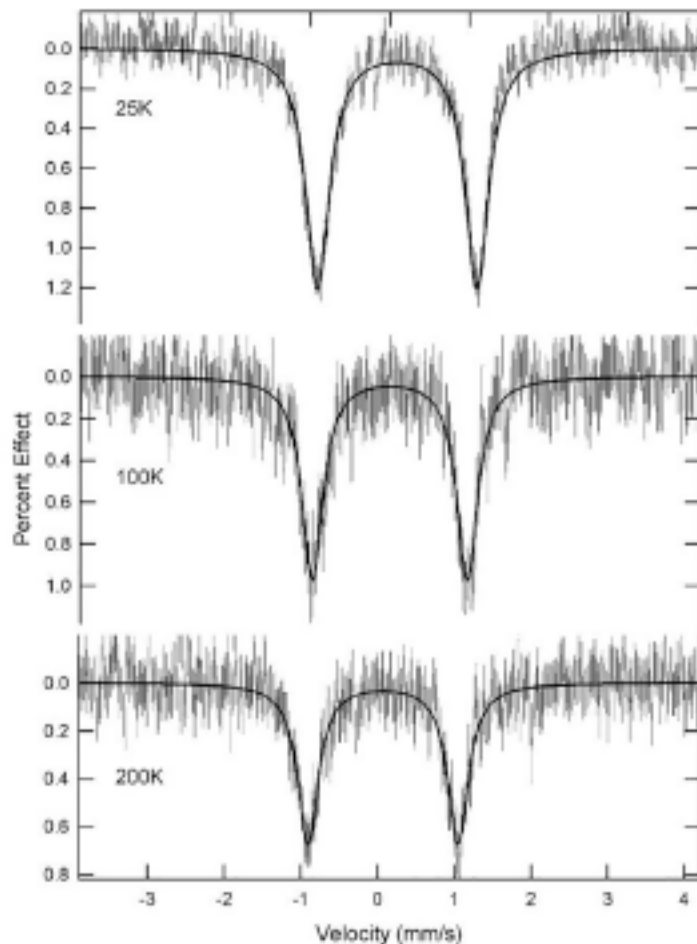


Fig. 6. Mössbauer spectra of $[\text{Fe}^{\text{III}}(\text{TMPP})(4\text{-CNpy})_2]\text{SO}_2\text{CF}_3 \cdot \text{C}_6\text{H}_5\text{Cl}$ (I) at 25 K, 100 K and 200 K in a weak applied magnetic field of 500 G. The solid lines are Lorentz fits to the data.

Individual values of displacements of the atoms from the mean plane of the 24-atom core (in units of 0.01 Å) of (I) are shown in Fig. 3. The average absolute displacement values of the *meso* carbon with respect to the plane of the 24 atoms of the porphyrin core (ΔC_{meso}), which measure the ruffling deformation of the porphyrin cycle, is also reported in Table 2, where we can notice that the Fe-Np distance decreases when the ring ruffling increases as just mentioned above. In Table 2 we can see that for the very ruffled porphyrin ring of the TPP-4-CNpy iron(III) derivative, with the highest ΔC_{meso} value of 0.55 Å, the Fe-Np distance value [1.952(4) Å] is the smallest among all the low-spin iron(III) metalloporphyrins reported in this table. For the other two iron(III)-bis(4-NCpy) species, the Fe-Np/ ΔC_{meso} values are 1.961(6)/0.41 and 1.971(2)/0.21 for the TMP and our TMPP derivative respectively, which confirms what we have just reported. Therefore, even though our TMPP derivative exhibits a less ruffled porphyrin core and a higher Fe-Np distance compared to the TPP and TMP derivatives, our iron(III) species can still be considered as presenting a highly ruffled porphyrin core and short Fe-Np distance. Based on the structural data, we can conclude that complex (I) belonging to the low-spin iron(III) hexacoordinated metalloporphyrins with the novel electronic configuration $(d_{xz}, d_{yz})^4(d_{xy})^1$.

For the TPP-bis(4-CNpy) species, the very high ruffling deformation and the very short Fe-Np distance are mainly due to an electronic effect where the 4-CNpy axial ligand is known to be a very strong π -acceptor ligand [11] while in the case of the TMP-bis(4-CNpy) compound, the steric effect of the porphyrin is the predominant cause of the high ruffling deformation of the porphyrin core and the short value of the Fe-Np distance [10]. In the case of our TMPP-bis(4-CNpy) complex (I), the donor effect of the methoxy groups in the *para* positions of the porphyrin phenyls destabilizes the π orbitals of the porphyrin core,

Table 3
List of hyperfine parameters of ^{57}Fe Mössbauer data and corresponding structural parameter ϕ for several low-spin Fe(III) porphyrin complexes.

Complex	T (K)	δ (mm/s)	ΔE_Q (mm/s)	ϕ (in $^\circ$) ^a	Ref.
[Fe ^{III} (OMTPP)(1-MeHIm) ₂]Cl ^{b,c}	77	0.28	2.78	10.5	[46]
[Fe ^{III} (OEP)(4-NMe ₂ py) ₂]ClO ₄ ^{d,e}	77	0.26	2.14	0	[10]
[Fe ^{III} (TMP)(4-NMe ₂ py) ₂]ClO ₄ ^{e,h}	77	0.20	1.74	90	[10]
[Fe ^{III} (TMP)(3-Etpy) ₂]ClO ₄ ^{f,g}	77	0.18	1.25	86	[47]
[Fe ^{III} (TMP)(3-Clpy) ₂]ClO ₄ ^h	77	0.20	1.96	88	[10]
[Fe ^{III} (TMP)(2-MeHIm) ₂]ClO ₄ ⁱ	77	0.20	1.48	88	[10]
[Fe ^{III} (TPP)(2-MeHIm) ₂]Cl ^j	150	0.22	1.77	90	[10]
[Fe ^{III} (TPP)(py) ₂]ClO ₄ ^k	77	0.16	1.25	86	[8]
[Fe ^{III} (PP)(py) ₂]Cl ^l	77	0.23	2.23	-	[48]
[Fe ^{III} (PP)(HIm) ₂]Cl ^{k,l}	77	0.13	2.27	-	[49]
[Fe ^{III} (PPD)(HIm) ₂]Cl ^{m,n}	77	0.24	2.35	-	[8]
[Fe ^{III} (TPP)(HIm) ₂]Cl ^l	77	0.23	2.23	0	[8]
[Fe ^{III} (PMXPP)(HIm) ₂]Cl ^o	298	0.13	2.27	-	[8]
[Fe ^{III} (PMXPP)(HIm) ₂]Br ^o	298	0.16	2.05	-	[8]
[Fe ^{III} (PCIPP)(HIm) ₂]Cl ^o	298	0.15	2.01	-	[8]
[Fe ^{III} (TPP)(4-CNpy) ₂]ClO ₄ ^p	120	0.19(1)	0.65(1)	88.97	[11]
[K(18-C-6)][Fe ^{III} (TPP)(CN) ₂].3CH ₂ Cl ₂ ^{q,r}	100	0.11	1.77	-	[45]
[K(2.2.2)][Fe ^{III} (TMP)(CN) ₂].3CH ₂ Cl ₂ ^{q,r}	298	0.09	0.35	-	[47]
[Fe ^{III} (TMP)(4-CNpy)]ClO ₄ ^p	77	0.20	0.97	87.41	[10]
[Fe ^{III} (TPP)(4-CNpy)]ClO ₄ ^p	120	0.19(1)	0.65(1)	88.97	[11]
[Fe ^{III} (TMPP)(4-CNpy)] ₂ SO ₂ CF ₃	25	0.089(5)	2.006(5)	72.6	This work
	100	0.095(1)	1.99(1)		
	200	0.07(1)	1.95(1)		

^a : ϕ = Dihedral angle between the two axial ligands (Relative orientation).

^b : OMTPP = octaalkyltetraphenylporphinato.

^c : 1-MeHIm = 1-methylimidazole.

^d : OEP = octaethylporphyrinato.

^e : 4-NMe₂py = 4-(dimethylamino)pyridine.

^f : TMP = meso-tetramesitylporphyrinato.

^g : 3-Etpy = 3-ethylpyridine.

^h : 3-Clpy = 3-chloropyridine.

ⁱ : 2-MeHIm = 2-methylimidazole.

^j : TPP = meso-tetraphenylporphyrinato.

^k : PP = Protoporphyrin IX.

^l : Him = imidazole.

^m : PPD = Protoporphyrin IX dimethyl ester.

ⁿ : PMXPP = meso-tetrakis(p-anisidyl)porphinato.

^o : PCIPP = meso-tetrakis(p-chlorophenyl)porphyrinato.

^p : 18-C-6 = 18-crown-6 = 1,4,7,10,13,16-hexaoxacyclooctadecane.

^q : 222 = Cryptand-222 = 4,7,13,16,21,24-hexaoxa-1,10-diazabicyclo[8.8.8]hexacosane.

especially the a_{2u} porphyrin HOMO orbital which has large density at the meso-positions. This is possible when the porphyrin core is very ruffled (Figs. 3 and 4) leading to destabilization of the d_{xy} orbital and makes the interaction between the half-filled d_{xy} and filled porphyrin a_{2u} HOMO orbital possible, leading to the novel electronic configuration $(d_{xz}, d_{yz})^4(d_{xy})^1$ [12].

Notably, Safo et al., [11] reported that more the greater the ruffling of the porphyrin core, the closer the dihedral angle ϕ (between the planes of the two N-donor planar axial ligands) is to 90° . Thus, for the very ruffled [Fe^{III}(TPP)(4-CNpy)₂]⁺ species, the ϕ value is 88.97° while the values of this angle are 87.41° for the TMP-bis(4-CNpy) derivative and 72.6° for our TMP-Pbis(4-CNpy) species (I). This is in accord with the amplitude of the ruffling distortions of these species.

The projection of the two 4-CNpy axial ligand planes are close to bisecting adjacent Np-Fe-Np angles where the pyridyl planes make dihedral angle (φ) values of 37.016° and 35.121° (Fig. 4) and lay over the meso positions of the porphyrin. These values are normal for hexa-coordinated iron(III) metalloporphyrins type [Fe^{III}(Porph)(L)₂]⁺ where L is a N-donor planar neutral ligand.

The dihedral angle between the mean porphyrin macrocycle of (I) and the pyridyl planes of the two trans 4-CNpy axial ligands are $86.52(7)^\circ$ and $86.49(9)^\circ$. These values are close to those of the TPP-bis(4-CNpy) ($87.14^\circ/85.08^\circ$) but quite higher than those of the TMP-bis(4-CNpy) related species ($82.74^\circ/75.79^\circ$). The phenyl planes of the TMPP porphyrinato are nearly perpendicular to the porphyrin core with

dihedral angles of 87.14° , 87.02° , 74.90° and 76.98° which are slightly higher than those of the two related ion complexes [Fe^{III}(TPP)(4-CNpy)₂]⁺ (58.50° , 66.99° , 60.09° , 66.98°) and [Fe^{III}(TMP)(4-CNpy)₂]⁺ (83.90° , 85.61° , 83.53° and 84.36°) where we notice once again that the TPP-4-CNpy derivative presents lower values than our TMPP-bis(4-CNpy) and the TMP-bis(4-CNpy) species.

The crystal packing of the title compound is made by a zigzag parallel layer perpendicular to the [1 0 0] direction (Fig. 5). Between these sheets are located the SO₂CF₃⁻ counterions and the chlorobenzene solvent molecules. One SO₂CF₃⁻ ion is weakly bonded to five neighboring [Fe^{III}(TMPP)(4-CNpy)₂]⁺ ion complexes: (i) the oxygen O5 of the SO₂CF₃⁻ anion, the carbon C53 of a phenyl group of one TMPP moiety and the carbon C46 of a methoxy group of a second TMPP porphyrinato are linked together by a non-conventional H bond C-H...O with a C53-H53...O5 and C46-H46A...O5 distance values of 3.513 (7) Å and 3.223 (6) Å respectively, (ii) the carbon C47 of a methoxy group of one TMPP and the carbon C51 of one 4-CNpy axial ligand of a nearby [Fe^{III}(TMPP)(4-CNpy)₂]⁺ ion are engaged in a weak non-conventional hydrogen C-H...O bond [distance = C53-H53...O5 = 3.513 (7) Å and distance = C46-H46A...O5 = 3.223 (6) Å], (iii) another weak C-H...O hydrogen bond links the oxygen O7 of the same triflate counterion to the carbon C59 of one 4-CNpy axial ligand with a C59-H59...O7 distance of 3.183 (7) Å, (iv) the fluorine atom F1 of the counterion and the centroid Cg2 of the pyrrole ring N2/C6-C9 of one TMPP porphyrin are weakly linked via the F...Cg non-bonding contact (Fig. SI-1, Tables SI-3-4) and

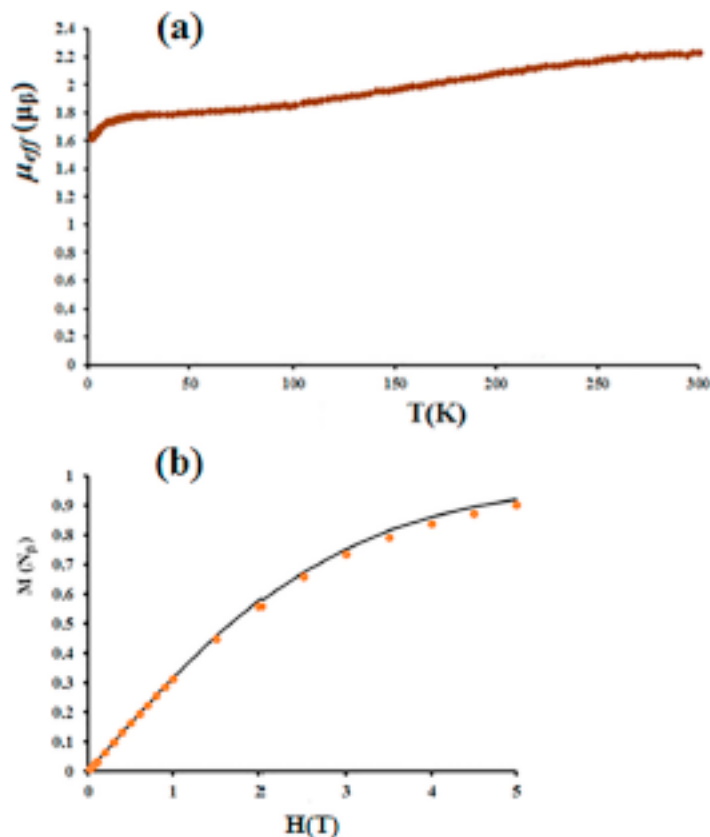


Fig. 7. (a): Temperature dependence of the effective magnetic moment μ_{eff} of (I). (b): The magnetization versus the applied magnetic field H at 2.0 K; (■): experimental data of (I) and (—): the Brillouin function with $g = 2$.

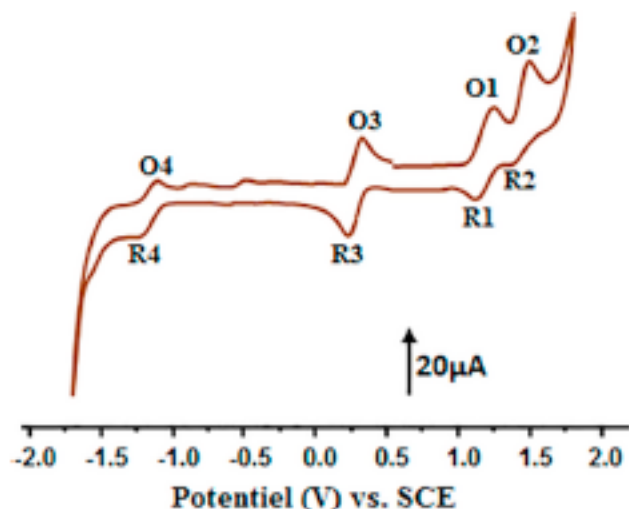


Fig. 8. Cyclic voltammogram of (I). The solvent is the dichloromethane and the concentration is ca. 10^{-2} M in 0.2M TBAPF₆, 100 mV/s, vitreous carbon working electrode ($\varnothing = 2$ mm).

(v) the fluorine F3 is engaged in a F \cdots Cg intermolecular interaction with the centroid Cg4 of the pyrrole ring N4/C16-C19 (Fig. S1-1, Tables S1-3-4). The centroid Cg2 is also linked to the chlorine atom of one chlorobenzene solvent molecule with a Cl \cdots Cg2 interaction value of 3.715 (2) Å.

3.3. Mössbauer investigation

The Mössbauer spectra of the polycrystalline [Fe^{III}(TMPP)(4-CNpy)₂]SO₂CF₃ (I) coordination compound were taken at 200 K, 100 K and 25 K and are illustrated in Fig. 6 while the Mössbauer data of (I) and several related iron(III) metalloporphyrins are summarized in Table 4. As was mentioned in the crystallographic section, iron(III) low-

spin porphyrinates exhibit two ground state configurations $(d_{xy})^2(d_{xz}, d_{yz})^3$ and $(d_{xz}, d_{yz})^4(d_{xy})^1$. Which group a compound belongs to depends on the steric and the donating-withdrawing effects of the groups at the phenyl rings of the porphyrin and also on the donating-withdrawing properties of the axial ligands.

It has been reported that quadrupole splitting (ΔE_Q) values of -1.75 mm.s⁻¹ are expected for low-spin ferric porphyrins with perpendicular axial ligand orientations and a pure $(d_{xz}, d_{yz})^4(d_{xy})^1$ ground state while values greater than -2.00 mm.s⁻¹ are typical for ferric species with parallel ligand orientations (Table 3) with the classic electronic configuration $(d_{xy})^2(d_{xz}, d_{yz})^3$. As shown in this table, the $\Delta E_Q/\delta$ values (δ is the isomeric shift) for our derivative are 2.006(5)/0.089(5), 1.99(1)/0.05(1) and 1.95(1)/0.07(1) mm.s⁻¹ at 25, 100 and 200 K respectively which indicates little if any temperature dependence. Given the values of the $\Delta E_Q - 2.00$ mm.s⁻¹, it is not clear based on the Mössbauer data, whether the electronic configuration of the ground state for the iron(III) of our model is $(d_{xy})^2(d_{xz}, d_{yz})^3$ or $(d_{xz}, d_{yz})^4(d_{xy})^1$, even though the crystallographic data are in favor of the latter electronic configuration.

For the related bis(4-CNpy) complexes, the $\Delta E_Q/\delta$ values are 0.97 mm.s⁻¹/0.20 mm.s⁻¹ and 0.65 mm.s⁻¹/0.19 mm.s⁻¹ for the TMP-bis(4-CNpy) and the TPP-bis(4-CNpy) derivatives respectively [10,11]. These two iron(III) complexes are considered low-spin and present the novel electronic configuration, and the value of -0.20 mm.s⁻¹ of the isomer shift is consistent with values commonly observed for low-spin ferric porphyrins. The quadrupole splitting value (0.97 mm.s⁻¹ at 77 K) of the [Fe^{III}(TMP)(4-CNpy)₂]⁺ ion complex is quite low but the [Fe^{III}(TPP)(4-CNpy)₂]⁺ species exhibits an unusual small ΔE_Q value of 0.65 mm.s⁻¹ as well. Safo et al., [11] explained such a small value of the quadrupole splitting as due to the fact that the orbital angular momentum of the metal center d-electrons is largely quenched, as is expected for a $(d_{xy})^2$ unpaired electron in a non-degenerate state. The isomer shift value of our TMPP-bis(4-CNpy) derivative, which is 0.095(1) mm.s⁻¹ at 100 K, is smaller than those found for the majority of hexa-coordinated low-spin iron(III) porphyrinates of type [Fe^{III}(Porph)(L)₂]⁺ (Porph = meso-porphyrinato and L is a neutral N-donor neutral axial ligand) with values of -0.20 mm.s⁻¹. This is the case of the TPP-bis(4-CNpy) and TMP-bis(4-CNpy) iron(III) related species with δ values of 0.19(1) mm.s⁻¹ and 0.20 mm.s⁻¹ respectively. It is noteworthy that the iron(III) bis(cyano)porphyrinates [Fe^{III}(TPP)(CN)₂]⁻ and [Fe^{III}(TMP)(CN)₂]⁻ [45] exhibit also small isomer shift values of 0.006 mm.s⁻¹ and 0.10 mm.s⁻¹ at 298 K respectively. Such low δ values are indicative of strong iron-axial ligand covalency.

In the same reference [45], Scheidt et al., based on Mössbauer data, deduced that the iron(III) low-spin bis(cyano) metalloporphyrins exhibits either the $(d_{xy})^2(d_{xz}, d_{yz})^3$ or the $(d_{xz}, d_{yz})^4(d_{xy})^1$ electronic configurations and that these configurations can be interconverted: the energy levels of the two ground state configurations are very close and that the nature of the porphyrin and the axial ligands as well as the cyanide ligand environment determine the type of the ground state electronic configuration of the iron(III).

3.4. Magnetic susceptibility measurements

Temperature dependent magnetic susceptibility measurements for (I) were performed on polycrystalline samples in the range 2–300 K using a SQUID magnetometer. In all cases, the magnetic susceptibility χ_M values have been corrected for diamagnetism [50]. Fig. 7-(a) illustrates the effective magnetic moment (μ_{eff}) versus the temperature of our [Fe(TMPP)(4-CNpy)₂]⁺ ion complex. As shown in this figure, there is a very small variation of the μ_{eff} values with temperature. Indeed, at 300 K the value of the effective magnetic moment is 2.23 μ_B while at 2.0 K the (μ_{eff}) value is 1.62 μ_B . Both values are appropriate for low-spin ($S = 1/2$) iron(III) compounds with $g = 2$. By the other hand, at room temperature, the product of molar susceptibility times temperature

Table 4
Electrochemical data^a for (I) and a selection of related low-spin iron(III) metalloporphyrins.

Complex	Oxidations	Reductions			Solvent	Ref.
	Ring oxidation $E_{1/2}^b$	Fe(III)/Fe(IV) $E_{1/2}^b$	Fe(III)/Fe(II) $E_{1/2}^b$	Fe(II)/Fe(I) $E_{1/2}^b$		
[Fe ^{III} (TPP)(1-Melm) ₂] ^{+c,d}	-	-	-0.16	-	CH ₂ Cl ₂	[52]
[Fe ^{III} (TPP)(py) ₂] ^{+c}	-	-	0.06	-	CH ₂ Cl ₂	[52]
[Fe ^{III} (OEP)(4-NH ₂ Py) ₂] ^{+e,f}	-	-	-0.39	-	CH ₂ Cl ₂	[52]
[Fe ^{III} (OEP)(pyz) ₂] ^{+g,h}	1.59	1.23	-0.50	-	CH ₂ Cl ₂	[53]
[Fe ^{III} (TFPP)(pyz) ₂] ^{+g,h}	1.43	1.19	0.32	-	CH ₂ Cl ₂	[54]
[Fe ^{III} (TCIPP)(pyz) ₂] ^{+g,h}	1.44	1.20	0.33	-	CH ₂ Cl ₂	[54]
<i>Iron(III) bis(4-cyanopyridine) metalloporphyrins</i>						
[Fe ^{III} (2,6-F ₂ -TPP)(4-CNpy) ₂] ⁺ⁱ	-	-	0.55	-	DMF	[52]
[Fe ^{III} (2,6-Br ₂ -TPP)(4-CNpy) ₂] ^{+k}	-	-	0.45	-	DMF	[52]
[Fe ^{III} (TPP)(4-CNpy) ₂] ^{+c,i}	-	-	0.31	-	DMF	[52]
[Fe ^{III} (TMP)(4-CNpy) ₂] ⁺ⁱ	-	-	0.33	-	DMF	[52]
[Fe ^{III} (2,6-OMe ₂ -TPP)(4-CNpy) ₂] ^{+m,n}	-	-	0.22	-	DMF	[52]
[Fe ^{III} (TMPP)(4-CNpy) ₂] ^{+ (I)}	1.44	1.18	0.28	-1.17	CH ₂ Cl ₂	This work

^a : the potentials are reported versus SCE.

^b : $E_{1/2}$ = half-wave potential.

^c : TPP = *meso*-tetraphenylporphyrinato.

^d : 1-Melm = 1-methylimidazole.

^e : OEP = octaethylporphyrinato.

^f : 4-NH₂Py = 4-(dimethylamino)pyridine.

^g : pyz = pyrazine.

^h : TFPP = *meso*-tetra(*para*-fluoro-phenyl)porphyrinato.

ⁱ : TCIPP = *meso*-tetra(*para*-chlorophenyl)porphyrinato.

^j : 2,6-F₂-TPP = *meso*-tetrakis(2,6-difluorophenyl)porphyrinato.

^k : 2,6-Br₂-TPP = *meso*-tetrakis(2,6-dibromophenyl)porphyrinato.

^l : irreversible wave.

^m : TMP = *meso*-tetramesitylporphyrinato.

ⁿ : 2,6-OMe₂-TPP = *meso*-tetrakis(2,6-dimethoxyphenyl)porphyrinato.

($\chi_M T$) of (I) is 0.60 which is higher than that of the spin-only value of 0.375 cm³.K.mol⁻¹ expected for one unpaired electron ($S = 1/2$) and characteristic of a moderate orbital contribution (Fig. S1-2). The ground state of the octahedral low-spin Fe(III) complexes is degenerate (²T_{2g} and a moderate orbital contribution to the $\chi_M T$ values is usually observed) [51].

In Fig. 5-(b), the field dependence of the magnetization, $M = f(H)$, at 2 K is shown where we can see that the experimental M values are compatible with the theoretical ones calculated using the Brillouin function with $S = 1/2$ ground state and $g = 2$.

3.5. Cyclic voltammetry

Cyclic voltammogram (CV) of complex (I) was recorded at room temperature in dichloromethane under an argon atmosphere in the potential range -2.0 to +2.0 V versus saturated calomel electrode (SCE) redox electrode with the tetra-*n*-butylammonium hexafluorophosphate (TBAPF₆) as the supporting electrolyte (0.2 M). The CV of our TMPP-bis(4-CNpy) iron(III) derivative is illustrated in Fig. 8 and values of half potential waves of (I) along with other related iron(III) metalloporphyrins are given in Table 4.

Complex (I) exhibits three reversible one electron oxidation waves and two reversible one electron reduction wave. The first wave (O1/R1) with a half wave potential value of 0.18 V is attributed to the Fe(III)/Fe(IV) oxidation while the oxidation wave (O2/R2) with an $E_{1/2}$ value of 1.44 V corresponding to the porphyrin ring oxidation. The first wave of the anodic part (R3/O3) of the CV of (I) with a $E_{1/2}$ value of 0.28 V is appropriate for the Fe(III)/Fe(II) reduction. The second wave (R4/O4) at $E_{1/2} = -1.17$ V is attributed to the reduction of the porphyrin rings.

It is noteworthy that several cyclic voltammetry investigations on low-spin iron(III) metalloporphyrins type [Fe^{III}(Porph)(L)₂]⁺ are reported in the literature [52,13]. Walker et al., [13], correlated the positive shift of the half wave potential values of the Fe(III)/Fe(II)

reduction of several bis(4-CNpy) low-spin iron(III) porphyrin complexes with the electron-donating/electron-withdrawing properties of the substituents at the phenyl rings of the porphyrin. Indeed, the same authors [13] classified the iron(III) bis(4-CNpy) in the order of the most easily reduced to the more difficult : 2,6-F₂-TPP > 2,6-TPP > 2,6-TMP > 2,6-OMe₂ [2,6-F₂-TPP = *meso*-tetrakis(2,6-difluorophenyl)porphyrinato, 2,6-TPP = *meso*-tetraphenylporphyrinato, 2,6-TMP = *meso*-tetramesitylporphyrinato and 2,6-OMe₂ = *meso*-tetrakis(2,6-dimethoxyphenyl)porphyrinato] which is approximately the order of electron-donating/electron-withdrawing capabilities of the substituents at the *ortho* positions of the phenyls of the porphyrin. Thus, the $E_{1/2}$ [Fe(III)/Fe(II)] values are 0.55 V, 0.31 V, 0.33 V and 0.22 V for the 2,6-F₂-TPP, 2,6-TPP, 2,6-TMP and 2,6-OMe₂ iron(III) porphyrin complexes in accordance with the increasing of the electron-donor character from the fluorine to the OCH₃ group. For our TMPP-Bis(4-CNpy) iron(III) species (which has an OMe donor group in the *para* position of the phenyls of the *meso*-porphyrin), the $E_{1/2}$ [Fe(III)/Fe(II)] value is 0.28 V indicating a negative shift compared to those of the TMP-bis(4-CNpy) and the TPP-bis(4-CNpy) derivatives with a half potential values of 0.33 V and 0.31 V respectively and more positive shift than that of the $E_{1/2}$ potential of the 2,6-OMe₂-bis(4-CNpy) species with a value of 0.22 V (which have two donor OMe groups in the *ortho* positions). All other things being equal, this is a confirmation of the important electron-donating/electron-withdrawing effect of the substituents at the phenyl rings of the porphyrin on the $E_{1/2}$ value of the Fe(III)/Fe(II) reduction of [Fe^{III}(Porph)(L)₂]⁺ ion complexes (Porph = *meso*-porphyrinato and L = *N*-donor planar axial ligand).

4. Conclusion

A new low-spin iron(III) bis(4-cyanopyridine), with the *meso*-tetraphenylporphyrin substituted at the phenyls *para* positions by the *o*-donor OMe group [complex (I)] was prepared and characterized. The

structural data of (I) indicates that the two 4-CNpy axial ligand adopt a perpendicular orientation. In the case of the iron(III) bis(4-CNpy) analogue complexes with the TPP and TMP porphyrinates which present also a perpendicular orientation of the axial ligands, they exhibit very short value of the average equatorial Fe-Np distance and a very high ruffling deformation of the porphyrin core. For the TPP species, this is explained by the very strong π -acceptor character of the 4-CNpy ligand while in the case of the TMP derivative, the steric effect of the porphyrin is the predominate cause of the high ruffling deformation porphyrin core and the short value of the Fe-Np distance. For our derivative, the Fe-Np bond length and the ruffling deformation are also high but smaller than those of the TPP and the TMP species.

This can be explained by the σ -donor character of the OMe group in the *para* positions of the *meso*-tetraarylporphyrin. From the structural data of (I), we can conclude that our synthetic species belongs to the low-spin iron(III) hexacoordinated metalloporphyrins with the ground state electronic configuration $(d_{xy})^4(d_{yz})^2$. The Mössbauer data of the relative of the related bis(CNpy)-iron(III) TPP and TMP coordination compounds, exhibit small values of the ΔE_Q value indicating that the ground state configuration of these metalloporphyrins is $(d_{xy})^4(d_{yz})^2$ which is not the case of our bis(CNpy)-iron(III)-TMPP complex for which the Mössbauer data are not conclusive concerning the type of the electronic configuration of the ground state.

The SQUID data of complex (I) confirm the low-spin $S = 1/2$ of the iron(III) with a small variation of the effective magnetic moment from 2.23 μ_B at 2.0 K the (μ_{eff}) value is 1.62 μ_B . The positive value of the half wave potential of the Fe(III)/Fe(II) reduction of 0.28 V of our *para*-OMe iron(III) bis(4-CNpy) (I) is very close to that of the related 2,6-OMe₂ complex (0.22 V) indicative of the important donating/withdrawing character of the phenyl substituents of the *meso*-porphyrin of the [Fe^{III}(*meso*-Porph)(4-CNpy)₂]⁺ ion complexes on the reduction of the Fe(III)/Fe(II) of these derivatives.

Acknowledgement

The authors gratefully acknowledge financial support from the Ministry of Higher Education and Scientific Research of Tunisia.

Appendix A. Supplementary data

Supplementary data to this article can be found online at <https://doi.org/10.1016/j.ica.2018.11.040>.

References

- [1] M. Pierrot, R. Haser, M. Frey, F. Payan, J.-P. Astier, *J. Biol. Chem.* 247 (1982) 14341.
- [2] F.S. Mathews, E.S. Czerwinski, P. Argos, in: Dolphin, D. (eds), *The porphyrins*, New York, 1979, Vol. VII, pp. 108.
- [3] C.F. Strickmatt, E.G. Ball, *Proc. Natl. Acad. Sci.* 38 (1952) 19.
- [4] G.T. Babcock, W.R. Widger, W.A. Cramer, W.A. Oertling, J.G. Metz, *Biochemistry* 24 (1985) 3638.
- [5] K. Niki, Y. Kawasaki, N. Nishimura, Y. Higuchi, N. Yasuoka, M. Kakudo, *J. Electroanal. Chem.* 168 (1984) 275.
- [6] D.K. Gelger, Y.J. Lee, W.R. Scheidt, *J. Am. Chem. Soc.* 106 (1984) 6339.
- [7] W.R. Scheidt, S.R. Osvald, Y.J. Lee, *J. Am. Chem. Soc.* 109 (1987) 1958.
- [8] D. Inniss, S.M. Solis, C.E. Strouse, *J. Am. Chem. Soc.* 110 (1988) 5644.

- [9] M.K. Safo, G.P. Gupta, F.A. Walker, W.R. Scheidt, *J. Am. Chem. Soc.* 113 (1991) 5497.
- [10] M.K. Safo, G.P. Gupta, C.T. Watson, U. Simonis, F.A. Walker, W.R. Scheidt, *J. Am. Chem. Soc.* 114 (1992) 7066.
- [11] M.K. Safo, F.A. Walker, A.M. Raitzström, W.P. Walters, D.P. Dolata, P.G. Debrunner, W.R. Scheidt, *J. Am. Chem. Soc.* 116 (1994) 7760.
- [12] M. Nakamura, Y. Obgo, A. Iwazaki, *J. Inorg. Biochem.* 102 (2008) 433.
- [13] M.J.M. Nessel, N.V. Shokhirev, P.D. Enemark, S.E. Jacobson, F.A. Walker, *Inorg. Chem.* 35 (1996) 5188.
- [14] M.J. Nappa, C.A. Tolman, *Inorg. Chem.* 24 (1985) 4711.
- [15] N.A. Stephenson, A.T. Bell, *Inorg. Chem.* 46 (2007) 2285.
- [16] S. Samania, P.K. Das, S. Chatterjee, K. Sengupta, B. Mondal, A. Dey, *Inorg. Chem.* 52 (2013) 12963.
- [17] P. Li, X. Zhang, C. Hou, Y. Chen, *Appl. Catal. B: Environ.* (2018), <https://doi.org/10.1016/j.apcath.2018.07.066> Accepted paper.
- [18] J. Chen, W.R. Browne, *Coord. Chem. Rev.* 374 (2018) 15.
- [19] S. Paul, F. Amalraj, S. Radhakrishnan, *Synth. Met.* 159 (2009) 1019.
- [20] A. Rusli, K. Datta, P. Ghosh, A. Mulchandani, M.D. Shrivast, *Mater. Lett.* 96 (2013) 38.
- [21] A.D. Adler, F.R. Longo, J.D. Finarelli, J. Goldmacher, J. Assour, L.A. Korsakoff, *J. Org. Chem.* 32 (1967) 476.
- [22] A. Gismelssed, E.L. Bominaer, E. Bill, A.X. Traubwein, H. Winkler, H. Nasri, P. Doppel, D. Mandor, J. Fischer, R. Weiss, *Inorg. Chem.* 29 (1990) 2741.
- [23] A. Earnshaw, *Introduction to Magnetochemistry*, first ed., Academic Press, New York, London, 1968, pp. 1-4.
- [24] Bruker, APEX2, SAINT and SADABS, Bruker AXS Inc., Madison, Wisconsin, USA, 2006.
- [25] L.J. Bourhis, O.V. Dolomanov, R.J. Gildea, J.A.K. Howard, H. Puschmann, *Acta Cryst. A71* (2015) 59.
- [26] L. Palatinus, G. Chapuis, *J. Appl. Cryst.* 40 (2007) 786.
- [27] G.M. Sheldrick, *Acta Cryst. C71* (2015) 8.
- [28] L.J. Farrugia, *J. Appl. Cryst.* 45 (2012) 854.
- [29] R. Weiss, J. Fischer, V. Büsch, V. Schünemann, M. Gardan, A.X. Traubwein, J.A. Shelton, C.P. Gros, A. Tabard, R. Guillard, *Inorg. Chim. Acta* 337 (2002) 223.
- [30] J. W. Buchler, in: D. Dolphin (ed.), *The Porphyrins*, Academic Press: New-York, Vol. I (1978), pp. 390-474.
- [31] C. Mchiri, N. Amkt, S. Jabli, T. Roisnel, Habib Nasri, *J. Mol. Struct.* 1154 (2018) 51.
- [32] L. Jiang, A.R. Zaregin, J.T. Engle, C. Mittal, C.S. Hartley, C.J. Ziegler, H. Wang, *Chem. Commun.* 48 (2012) 6927.
- [33] W.R. Scheidt, C.A. Reed, *Chem. Rev.* 81 (1981) 543.
- [34] L.A. Yatsunyk, M.D. Carducci, F.A. Walker, *J. Am. Chem. Soc.* 125 (2003) 15986.
- [35] D.M. Collins, W.R. Scheidt, J.L. Hoard, *J. Am. Chem. Soc.* 94 (1972) 6689.
- [36] W.R. Scheidt, M.G. Finnegan, *Acta Crystallogr., Sect. C: Cryst. Struct. Commun.* C45 (1989) 1214.
- [37] H. Oumous, C. Levombo, J. Protas, P. Coccolis, R. Guillard, *Polyhedron* 3 (1984) 651.
- [38] M.S. Belkhiria, M. Dhifet, H. Nasri, *J. Porphyrins Phthalocyanines* 9 (2006) 575.
- [39] M.E. Kastner, W.R. Scheidt, T. Mashiko, C.A. Reed, *J. Am. Chem. Soc.* 100 (1978) 666.
- [40] W.R. Scheidt, Y.J. Lee, D.K. Gelger, K. Taylor, K. Hatano, *J. Am. Chem. Soc.* 104 (1982) 3367.
- [41] W.R. Scheidt, Y.J. Lee, *J. Am. Chem. Soc.* 105 (1983) 778.
- [42] M. Mykraj, L.A. Andersson, J. Sun, T.M. Loehr, C.A. Thomas, E.P. Sullivan, M.A. Thomson, K.M. Long, O.P. Anderson, *Inorg. Chem.* 34 (1995) 3963.
- [43] W.R. Scheidt, J.F. Kirner, J.L. Hoard, C.A. Reed, *J. Am. Chem. Soc.* 109 (1987) 1963.
- [44] W.R. Scheidt, K.J. Haller, K. Hatano, *J. Am. Chem. Soc.* 102 (1980) 3017.
- [45] J. Li, B.C. Noll, C.E. Schultz, W.R. Scheidt, *Inorg. Chem.* 54 (2015) 6472.
- [46] T. Teschner, L. Yatsunyk, V. Schünemann, H. Paulsen, H. Winkler, C. Hu, W.R. Scheidt, F.A. Walker, A.X. Traubwein, *J. Am. Chem. Soc.* 128 (2006) 1379.
- [47] D.A. Summerville, I.A. Cohen, K. Hatano, W.R. Scheidt, *Inorg. Chem.* 17 (1978) 2906.
- [48] D.K. Straub, W.M. Connor, *Ann. N. Y. Acad. Sci.* 206 (1973) 383.
- [49] L. Bullard, R.M. Panayappan, A.N. Thorpe, P. Hambright, A.G. Ng, *Biolnorg. Chem.* 3 (1974) 161.
- [50] M.F. Tweedle, L.J. Wilson, *J. Am. Chem. Soc.* 98 (1976) 4824.
- [51] J.C. Novaron, R. Herradora, M.M. Olmstead, P.K. Mascharak, *Inorg. Chim. Acta* 285 (1999) 269.
- [52] K.M. Kadish, C.H. Su, *J. Am. Chem. Soc.* 105 (1983) 177.
- [53] W.R. Scheidt, D.K. Gelger, K.J. Haller, *J. Am. Chem. Soc.* 104 (1982) 495.
- [54] S. Dhifaoui, S. Nasri, G. Gortard, A.C. Ghosh, Y. Garcia, C. Bonifacio, S. Najmudin, V. Marvaud, Habib Nasri, *Inorg. Chim. Acta* 477 (2015) 114.